Structures and energetics of Pt, Pd, and Ni adatom clusters on the Pt(001) surface: Embedded-atom-method calculations

Alan F. Wright
University of California, Davis, California 95616

Murray S. Daw
Sandia National Laboratories, Livermore, California 94550

C. Y. Fong
University of California, Davis, California 95616

(Received 2 July 1990)

The structures and energetics of Pt, Pd, and Ni adatom clusters on the Pt(001) surface have been investigated using the embedded-atom method (EAM). The stable configurations of Pt clusters are predicted to be linear chains oriented along the ⟨110⟩ directions for three and five adatoms and close-packed islands for four and six or more adatoms. These results are in agreement with a recent field-ion-microscopy (FIM) study and with previous EAM calculations [Schwoebel *et al.*, Phys. Rev. B **40**, 10 639 (1989)]. For Pd, the stable configurations are predicted to be close-packed islands except for three adatoms, for which a linear chain is the predicted stable configuration. Preliminary FIM observations, with Pd clusters containing up to six adatoms, agree with these predictions for four, five, and six adatoms, but are not conclusive concerning the stable configuration for three adatoms [G. L. Kellogg (private communication)]. For Ni, the stable configurations are predicted to be linear chains for all numbers of adatoms, and at this time no experimental observations have been reported. The similarities and differences in the results for Pt, Pd, and Ni adatoms are discussed, as well as the importance of substrate relaxations.

I. INTRODUCTION

A reliable description of the energetics of adatoms on surfaces is fundamental to modeling a surface process such as crystal growth from the vapor phase. An early step in this process is believed to be the formation of small adatom clusters which then serve as nucleation centers for the growth of a subsequent crystal layer. These clusters can be observed with field-ion microscopy (FIM) and their stable configurations, in turn, reflect features of the adatom-adatom and adatom-substrate interactions.

FIM studies have yielded the interesting result that the stable configurations of small adatom clusters are sometimes linear chains instead of close-packed, two-dimensional islands. For example, the stable configurations of small Ni, Pd, Pt, and Ir clusters on W(110) are linear chains oriented along the ⟨111⟩ directions.[1–3] With increasing numbers of adatoms, transitions to close-packed islands occur for Ni and Pd,[2,3] while Pt and Ir form structures consisting of intersecting linear chains.[1,2] Recently, linear chains oriented along the ⟨110⟩ directions have also been observed for Ir adatom on Ir(001) (Ref. 4) and Pt adatoms on Pt(001).[5] The latter system demonstrated an additional interesting behavior; the stable configurations were chains for three and five adatoms and islands for four, six, and seven adatoms. Furthermore, embedded-atom-method (EAM) calculations, performed as part of the investigation into the Pt on Pt(001) system, predicted these stable configurations and also indicated that substrate relaxations were important.[5]

Early theoretical attempts to describe the interactions of chemisorbed atoms on a metal surface relied primarily on Anderson-model calculations.[6–9] These studies demonstrated the existence of an indirect adatom-adatom interaction due to the coupling of the adatoms' electronic states through the substrate, and were qualitatively able to explain the existence of ordered overlayers of adatoms on metal surfaces. The application of electronic structure techniques to describe chemisorption systems has been limited mainly because of the computational effort required to adequately describe the substrate. In particular, a substrate in which there are significant relaxations would not be a good candidate for this type of approach. Nevertheless, advances in electronic structure techniques such as the class introduced by Car and Parrinello[10] and the first-principles scattering-theory method,[11] may soon make it possible to perform first-principles calculations of cluster energetics for some systems.

Because of the limitations of electronic structure techniques, semiempirical methods provide the most reasonable approach for systematic studies of adatom clusters on surfaces. The EAM has proven to be a reliable, semiempirical method for studying defects and surfaces of metals, and the success of the EAM in describing the stable configurations of Pt clusters on Pt(001) merits further work along these lines. Therefore the objective of

the present study is to expand on the previous EAM study of Pt clusters on Pt(001), and also to study Pd and Ni clusters on Pt(001). Primarily, we are interested in the predictions of the stable configurations for isolated adatom clusters. These predictions can be directly compared with FIM observations. Furthermore, we will investigate substrate relaxations, especially in terms of their influence on cluster stabilities.

The remainder of this paper is organized as follows: In Sec. II we describe the EAM, the qualitative nature of adatom-adatom interactions within the EAM, and the slab geometries used in our calculations. In Sec. III we discuss the predicted stable cluster configurations and the role of substrate relaxations, and we examine the adatom interactions. We present a brief summary in Sec. IV.

II. METHODS

A. Adatom-adatom interactions and the embedded-atom method

The EAM (Refs. 12 and 13) is a semiempirical, many-atom potential for computing the total energy of a metallic system. The method is appropriate for metals with empty or filled d bands and is especially useful for systems with large unit cells. In this approach, the energy of the metal is viewed as a sum of the energies obtained by embedding each atom into the local electron density provided by the remaining atoms of the system. In addition, there is an electrostatic interaction. The cohesive energy for a system of atoms is given by

$$E_{\rm coh}=\sum_i G_i\left[\sum_{j\neq i}\rho_j^a(R_{ij})\right]+\tfrac{1}{2}\sum_{i,j(j\neq i)}U_{ij}(R_{ij})\ , \tag{1}$$

where G is the embedding energy, ρ^a is the spherically averaged atomic electron density, R is the distance between atoms, and U is the electrostatic interaction. The embedding energy for an atom is defined as the interaction of that atom with the background electron density. The background density for an atom is determined by evaluating at its nucleus the superposition of atomic density tails from the other atoms. The forms of the embedding functions and electrostatic interactions are not unique, and in these calculations we have used the empirical set of embedding functions and electrostatic interactions developed in Ref. 13. These functions were fit to the following *bulk* properties: lattice constant, cohesive energy, elastic constants, vacancy formation energy, and dilute heats of alloying. No use of surface data was made during the determination of the functions. We also mention that it is possible to derive the EAM form from approximations made within density-functional theory.[14]

The EAM is currently the method of choice for doing semiempirical calculations in close-packed metals; it combines the computational simplicity needed for larger systems with a physical picture which includes certain many-atom effects and avoids some of the problems of the pair potential scheme. This method has been applied successfully to a variety of bulk and interface problems. The EAM has also been applied to several surface problems, such as surface structure,[12,13] surface reconstruction,[15,16] surface structural order-disorder transitions,[17] segregation to surfaces,[18,19] and surface ordered alloys.[20,21]

Obvious drawbacks of the EAM include non-self-consistent charge densities and the lack of a detailed description of electronic states. In particular, because the EAM does not deal with Fermi surfaces, interactions between adatoms will not include the long-range Friedel oscillations described in previous treatments.

On the other hand, a particularly appealing aspect of the EAM is its physical picture of metallic bonding. Each atom is embedded in a host electron gas created by its neighboring atoms. The atom-host interaction is described in a way that is inherently more complex than the simple pair-bond model. In this way, the embedding function incorporates some important many-atom interactions. It is then possible to describe and understand interatomic interactions on surfaces in terms of either the embedding function or the effective many-atom interactions that arise from it. In particular, it is simple to demonstrate how bonding is affected by coordination, and this naturally leads to an understanding of the difference between bulk and surface bonds. In the same way, we can also form a picture of substrate-mediated interactions and the role of substrate relaxations.

Although the EAM form is calculationally convenient, it is often conceptually useful to visualize effective N-atom interactions. These approximate interactions are qualitatively useful, but may not quantitatively represent the EAM results over a wide range of situations. The effective two- and three-atom interactions are given by[22]

$$\psi_{ij}(R)\equiv\tfrac{1}{2}\{[U_{ij}(R)+2G_i'(\bar\rho_i)\rho_j^a(R)+G_i''(\bar\rho_i)\rho_j^a(R)^2]+(i\leftrightarrow j)\}\ , \tag{2a}$$

$$\chi_{ijk}(R_i,R_j,R_k)\equiv[G_i''(\bar\rho_i)\rho_j^a(R_{ij})\rho_k^a(R_{ik})+(jki)+(kij)]\ , \tag{2b}$$

where $\bar\rho$ is the background density of a reference state, such as a perfect bulk lattice. Higher-body interactions can be obtained as well. Note that the effective interactions depend only on the distances between the atoms and not (explicitly) on any angles. This property of the EAM is a direct result of the form of Eq. (1).

The effective interactions in Eqs. (2) demonstrate that the interactions within the EAM are *environmental dependent,* in that the interaction between two atoms depends on the derivatives of their embedding functions, which depend on the $\bar\rho$ for each atom. As one approaches a surface, the effective two-atom interaction becomes stronger and the bond length shortens. Within the EAM, this is a result of the requirement that $G''>0$. In this way, the EAM describes the effect of coordination of bond strength: the less-coordinated surface atoms tend to have stronger bonds and shorter bond lengths. This, in fact, is the strength of EAM, and is directly connected to the nonlinearity of the embedding function. If one sets $G''=0$ (and $G'=$const) in Eqs. (2), then χ vanishes and the EAM can be replaced by a pair potential model based on $\psi(R)$. Thus the EAM contains pair potentials as a special case.

Another consequence of the positive second derivative of the embedding function ($G''>0$) is that the effective three-atom interaction χ is always repulsive. Also, notice that it is the sum of three terms each of which depends only on two bond lengths and no angles. It is this lack of angular dependence which makes the EAM in its present form less applicable to metals from the center of the transition series.[23]

Consider now the specific example of the interaction between two Pd adatoms in fourfold sites on a Pt(001) surface. The effective two-body interaction ψ contributes a direct attraction between the two adatoms. There are also effective three-body interactions, χ, formed from the triangles involving two Pd adatoms and a substrate atom. These contribute a repulsion to the interaction between the two adatoms. Thus the EAM naturally leads to the prediction of a substrate-mediated, adatom-adatom interaction. Specifically, our results will show that two Pd adatoms experience an attractive interaction at first near-neighbor sites; this attraction is largely due to the direct two-body attraction. However, we will also see that the two Pd adatoms experience a repulsive interaction at *second* near-neighbor sites. In this case, the direct two-body attraction is weakened by the larger bond distance, but the repulsive three-body effective interactions occur at nearly the same bond lengths.

The nature of this adatom-adatom interaction is quite different from that investigated by other workers.[8,24–26] In the EAM, the significant adatom-adatom interactions are short ranged, being most significant when two adatoms neighbor the same substrate atom. However, because we allow substrate relaxations, there will also be adatom-adatom interactions due to distortion of the substrate.

As with semiempirical calculations in general, our emphasis in this paper will be on general trends: trends with cluster size and adatom type. However, as we will see, semiquantitative agreement with experiment occurs in many cases.

B. Slab calculations

We performed our calculations using two-dimensional periodic slabs with surfaces perpendicular to the [001] direction. Three different slabs were used corresponding to the three types of calculations we performed, and the dimensions of the slabs were chosen so that the total energies were converged to within ± 0.001 eV.

(1) For calculations with adatom clusters, we used a 23-layer slab. The periodic vectors were along the [100] and [010] directions with lengths $16a$ ($a=3.92$ Å, the bulk lattice constant of Pt).

(2) For calculations with periodic chains of adatoms, we used a 50-layer slab. The periodic vectors were along the [110] and [1$\bar{1}$0] directions with lengths $4(a/\sqrt{2})$ and $50(a/\sqrt{2})$, respectively.

(3) For calculations with monolayer coverages of adatoms, we used a 25-layer slab. The periodic vectors were along the [100] and [010] directions with lengths $4a$.

The atoms in a slab were initially arranged as in bulk terminated Pt. We then used the EAM together with a conjugate gradients procedure[27] to relax the slab (without adatoms) to the minimum energy configuration. During this relaxation, the bottom four layers and the periodic lengths were held fixed. The atoms near the top surface (the relaxed surface) moved along the [001] direction; the first layer relaxed inward by 0.123 Å, the second layer relaxed outward by 0.012 Å, and the rest of the layers moved by less than 0.001 Å. These relaxed slabs then provided the starting points for all of the calculations with adatoms.

For the calculations with adatoms, the adatoms were initially placed at 1.25 Å above the fourfold sites of the relaxed surface. For example, in Fig. 1 we show the initial positions for a five-adatom linear chain and a five-adatom close-packed island. We then relaxed the substrate atoms and the adatoms to the minimum energy configuration, again holding the bottom four layers and the periodic lengths fixed. In general, the adatoms remained near their initial positions and the nearby substrate atoms relaxed away from the adatoms. To gauge the importance of these substrate relaxations, we also performed calculations on a frozen slab. For these calculations, adatoms were initially placed 1.25 Å above the fourfold sites of the relaxed surface as before. We then relaxed *just the adatoms* to the minimum energy configuration, holding all of the layers and the periodic lengths fixed.

Note that while reconstructions are known to occur for the Pt(001) surface,[28,29] we will compare our results with FIM studies in which the surfaces were not reconstructed.[30] (The surfaces used in the FIM studies were produced by field evaporation of atoms from the field-ion mi-

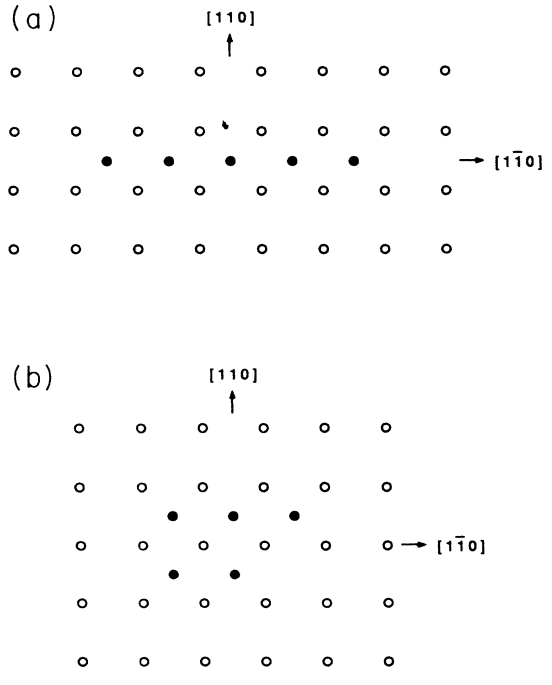

FIG. 1. Initial configurations, as viewed from above, of the first-layer substrate atoms (open circles) and the adatoms (solid circles) for (a) a five-adatom chain, and (b) a five-adatom island.

croscope tip and were not subsequently thermally equilibrated to produce a reconstruction.) Accordingly, although surface reconstructions could be investigated with the EAM, the calculations reported here were performed on an unreconstructed surface. Also, we have not considered three-dimensional adatom clusters. These could be treated with the EAM, however, the FIM studies show that small adatom clusters assume one- and two-dimensional configurations.

III. RESULTS

A. Stable cluster configurations

Our main objective was to find the stable configurations for small adatom clusters. To do this, we chose a set of configurations for each number of adatoms and then calculated the energy for each configuration and adatom type. As an example, in Fig. 2 we list the energies of the five-adatom Pt clusters. In this case, we predict that a chain is the stable (lowest-energy) configuration. While there are certainly other possible five-adatom configurations, we feel that this set is extensive enough so that we have found the lowest-energy configuration. Before showing the rest of our results, we mention that the energies listed in Fig. 2 are binding energies referred to isolated adatoms. For example, the (binding) energy of a five-adatom chain is given by

$$E_{C5,B}=(E_{C5}-E_{\text{slab}})-5(E_1-E_{\text{slab}})\ , \tag{3}$$

where E_{C5} is the total energy of the slab with the five-adatom chain, E_{slab} is the total energy of the slab with no adatoms, and E_1 is the total energy of the slab with one adatom. The calculated one-adatom adsorption energies, $|E_1-E_{\text{slab}}|$, are 5.230, 3.641, and 4.609 eV, respectively, for Pt, Pd, and Ni. (We will quote results to the nearest meV. We do not believe that the EAM is that accurate. Rather, some quantities of interest are that small.)

We considered clusters containing up to nine adatoms. The predicted stable configurations and their energies are listed in Fig. 3. Note that these configurations fall into two categories: (1) linear chains oriented along the ⟨110⟩ directions and (2) close-packed islands. Because of this,

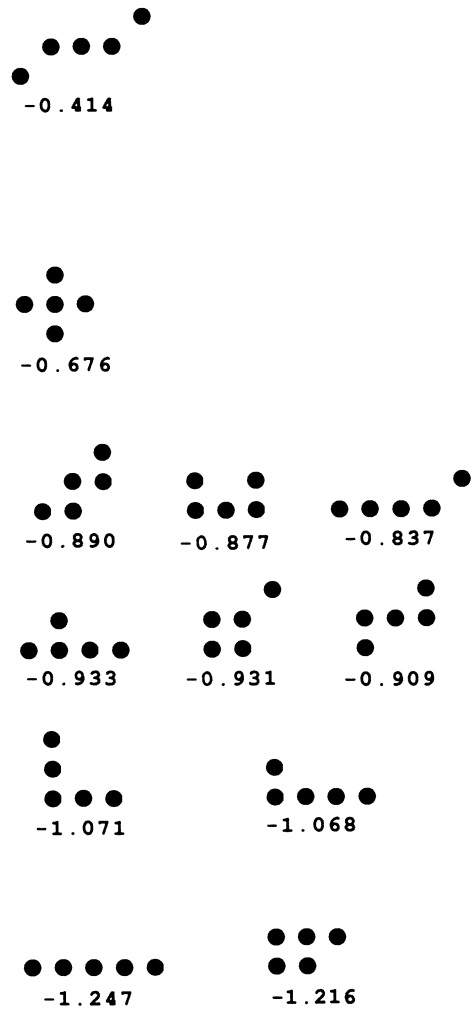

FIG. 2. The set of five-adatom configurations that we considered, and their energies calculated with Pt adatoms. The energies are in eV and are referred to isolated adatoms.

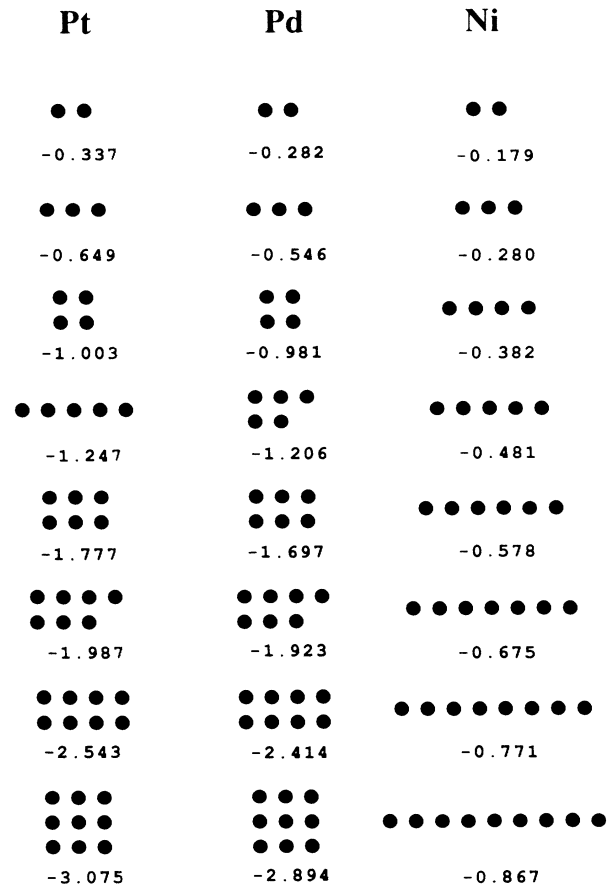

FIG. 3. Predicted stable configurations and their energies for Pt, Pd, and Ni clusters containing from two to nine adatoms. The energies are in eV and are referred to isolated adatoms. The predicted stable configurations for Pt clusters containing from two to seven adatoms were reported previously in Ref. 5.

we will pay particular attention to chains and islands throughout our analysis.

For Pt, our results are in agreement with the previous theoretical and experimental study of Pt on Pt(001) which considered clusters containing up to seven adatoms.[5] In particular, note the alternation between chain and island configurations for the smaller clusters; we predict that chains are stable for three and five adatoms and islands are stable for four and six adatoms. For larger clusters, we predict that islands are the stable configurations.

The results for Pd are identical to those for Pt, except that the predicted stable configuration for five adatoms is an island. The energies of the Pt and Pd clusters are also similar. Preliminary FIM observations of Pd on Pt(001) have been performed for clusters containing up to six adatoms.[30] The observed stable configurations for four, five, and six adatoms agree with our predictions, while for three adatoms the observations are not conclusive concerning the stable configuration.

The results for Ni are quite different. We predict that the stable configurations are chains for all numbers of adatoms. In addition, the energies are smaller than those of Pt and Pd clusters by a factor of about 3. This predicted stability of chains over islands for Ni results from two effects: (1) the different substrate relaxation energies for

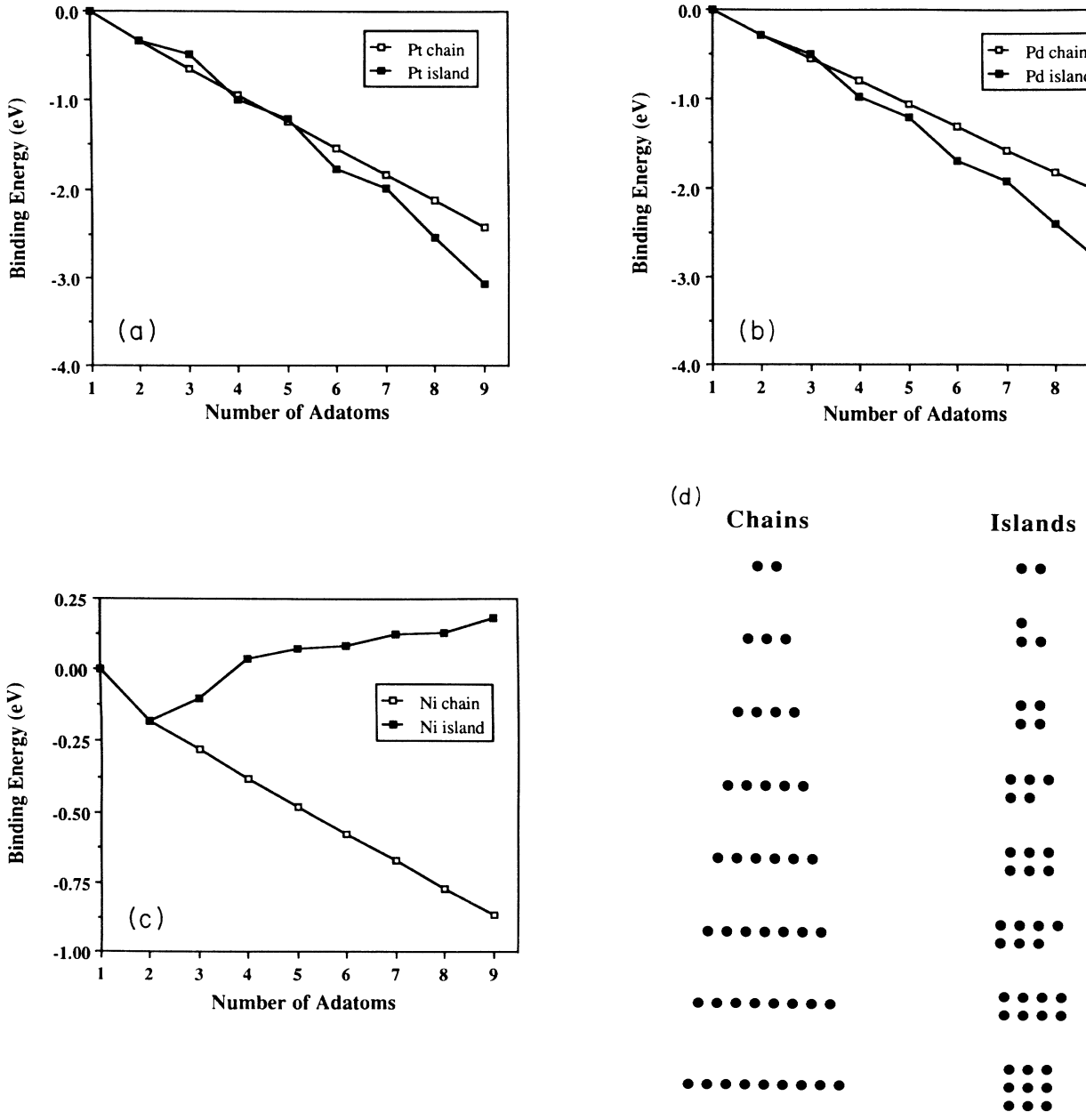

FIG. 4. Energies of the chain and island configurations shown in (d) for (a) Pt, (b) Pd, and (c) Ni adatoms on a relaxed slab. The energies are in eV and are referred to the isolated adatoms.

chains and islands and (2) the relatively weak first near-neighbor pair interaction between Ni adatoms. We will examine these two effects in detail in Secs. III B and III C, respectively, after we consider what our results imply for larger clusters. To our knowledge, there have been no conclusive experimental observations of the stable configurations of Ni clusters on Pt(001). However, there is an indication that Ni adatoms can exchange positions with the substrate atoms.[31] This is a possibility that we have not considered in this study, although it can be investigated using the EAM.

We did not calculate the energies of clusters containing more than nine adatoms, however, our results do provide some insight into their stable configurations. Specifically, we consider two questions: (1) Do islands continue to be stable with respect to chains for larger Pt and Pd clusters? and (2) Do chains continue to be stable with respect to islands for larger Ni clusters?

To answer the first question, we refer to Figs. 4(a) and 4(b). In Fig. 4(a) we plot the energies of Pt chains and islands versus the number of adatoms. The energy of a chain has nearly a linear dependence on the number of adatoms, while the energy of an island has a stairlike dependence. For small clusters, we see that the energies of chains and islands are similar and the stable configuration alternates between a chain and an island. However, at about six adatoms the energy difference between chains and islands begins to increase, with islands becoming increasingly stable with respect to chains. This corresponds to the transition from chain to island configurations which has been observed in FIM studies. From Fig. 4(a), it is clear that islands will continue to be stable with respect to chains for clusters containing more than nine adatoms. In Fig. 4(b), we plot the energies of Pd chains and islands versus the number of adatoms. The plots are similar to those for Pt except that the energy difference between chains and islands begins to increase at about four adatoms. Again, it is clear that islands will continue to be stable with respect to chains.

To answer the second question, we refer to Fig. 4(c), where we plot the energies of Ni chains and islands versus the number of adatoms. The energy of a chain has a nearly linear dependence on the number of adatoms as we saw for Pt and Pd. However, the energies of islands containing more than three adatoms are positive, indicating that they are unstable with respect to isolated adatoms. This lack of stability for Ni islands is due to the detailed nature of the adatom interactions which we will discuss later. Nevertheless, from Fig. 4(c) it is clear that chains will continue to be stable with respect to islands for Ni clusters containing more than nine adatoms. In particular then, our results predict that there will not be a transition from chain to island configurations as the number of adatoms increases.

Another feature to note from the binding energies (in Fig. 3) is that the larger clusters are stable with respect to smaller isolated clusters. For example, the sum of the energies of the four- and five-adatom Pt clusters is higher than the energy of the nine-adatom Pt cluster by 0.825 eV. To see whether this will be the case for clusters containing more than nine adatoms we again refer to Figs. 4(a)–4(c).

For Ni, consider the plot of the energies of chains versus the number of adatoms [Fig. 4(c)]. The slope of this curve converges, for about nine adatoms, to -0.095 eV/adatom. For comparison, we performed a calculation with widely separated, periodic chains of Ni adatoms. The energy per adatom for the periodic chain, $\varepsilon_{C,B}$ was also found to be -0.095 eV/adatom, indicating that the adatoms in the middle of a long chain are not influenced very much by the ends. This leads us to define a termination energy for a Ni chain,

$$E_T=\tfrac{1}{2}(E_{C9,B}-9\varepsilon_{C,B}) , \tag{4}$$

where $E_{C9,B}$ is the energy of the nine-adatom chain. This termination energy is negative, $E_T=-0.007$ eV, which indicates that longer Ni chains will be unstable with respect to shorter ones. For example, the energy of a 12-adatom chain ($E_{C12,B}=12\varepsilon_C+2E_T$) is slightly higher than the sum of the energies of two isolated six-adatom chains.

We also calculated termination energies for Pt and Pd chains. In contrast to Ni, these are positive: $+0.105$ and $+0.094$ eV, respectively, for Pt and Pd. It is interesting to note that, as with the stable cluster configurations, the results for Pt and Pd are similar.

With regard to Pt or Pd islands, we cannot calculate an edge energy analogous to the termination energy we calculated for chains. This is because the islands we have considered are too small. However, we can show that these edge energies will be positive. To do this we take the energy per adatom for a periodic monolayer and compare it to the energies per adatom for the islands. The energy per adatom for a periodic monolayer is -0.540 eV for Pt and -0.487 eV for Pd. These asymptotic energies are less than the energies per adatom for the islands that we have considered. This indicates that the edge energies will be positive and thus large islands will be stable with respect to smaller isolated islands.

B. Substrate relaxations

In the previous EAM study of the stable configurations of Pt clusters on Pt(001), Schwoebel *et al.* noted that inclusion of substrate relaxations was necessary in order to obtain agreement with the FIM observations.[5] In particular, they found that the predicted stable configurations on a frozen substrate were islands (instead of chains) for three and five adatoms. We have found that in addition to Pt, the predicted stable configurations of Pd and Ni clusters also depend on substrate relaxations. To demonstrate this dependence, it is sufficient to look at the energies of chains and islands on a frozen substrate [Figs. 5(a)–5(c)].

For Pt [Fig. 5(a)], we see that clusters on a frozen substrate are more stable as islands than as chains. In particular, chains are no longer the stable configurations for three and five adatoms, contrary to the FIM observations. Similar results are seen for Pd clusters on a frozen substrate [Fig. 5(b)] where a chain is no longer the stable configuration for three adatoms (the island energy is 0.020 eV lower than the chain energy for three adatoms).

For Ni [Fig. 5(c)], chains are no longer the stable configurations for four, six, eight, and nine adatoms without substrate relaxations.

By comparing the energies of chains and islands on a frozen substrate [Figs. 5(a)–5(c)] with their energies on a relaxed substrate [Figs. 4(a)–4(c)] we note that there is a common feature for the three types of adatoms. In each case, substrate relaxations lower the energies of chains with respect to islands. This effect is shown clearly in Figs. 6(a)–6(c) where we plot the relaxation energies of

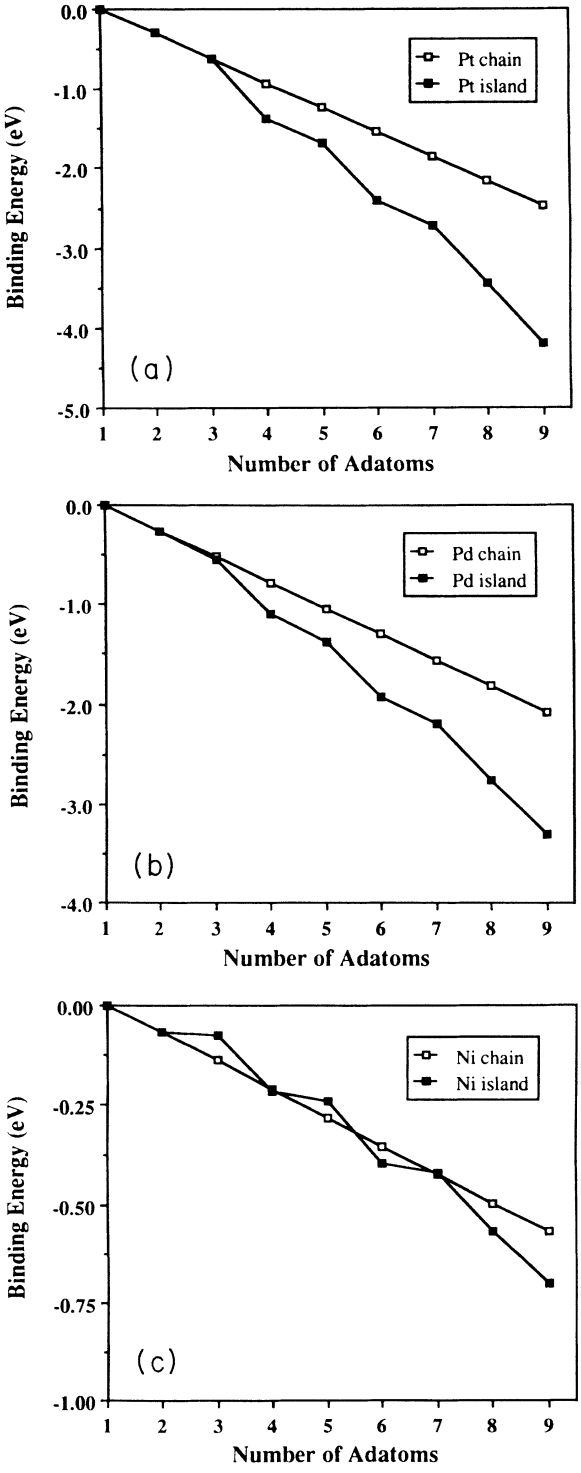

FIG. 5. Energies of the chain and island configurations shown in Fig. 4(d) for (a) Pt, (b) Pd, and (c) Ni adatoms on a frozen slab. The energies are in eV and are referred to isolated adatoms.

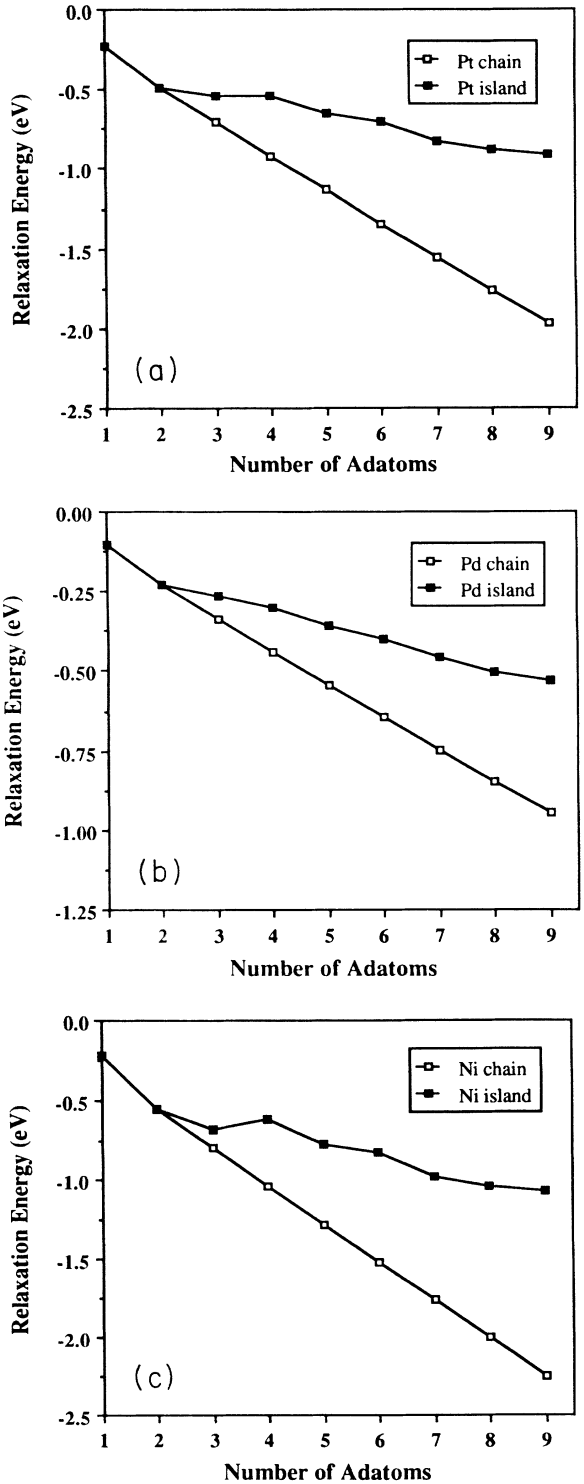

FIG. 6. Relaxation energies of the chain and island configurations shown in Fig. 4(d) for (a) Pt, (b) Pd, and (c) Ni. The energies are in eV.

chains and islands. (We define the relaxation energy for a cluster as the difference between the total energies calculated with relaxed and frozen substrates.) For each type of adatom, we see that the relaxation energy for a chain is about twice as large as for an island. Qualitatively, the origin of the larger relaxation energies for chains is easy to understand. We expect that relaxation takes place mainly around the circumference of a cluster and within the first layer of the substrate. Since an N-adatom chain has a larger circumference than an N-adatom island, we expect that the relaxation energy for a chain should be larger than for an island. In particular, for large islands the relaxation energy should have a $\sqrt{N}$ dependence while for chains, the dependence should be linear in N.

In the remainder of this section we will describe the main features of the substrate relaxations which occur for three configurations of Pt adatoms: (1) a single adatom, (2) a four-adatom chain, and (3) a four-adatom (square) island. In particular, we want to point out the qualitative differences in the substrate relaxations for chains and islands. Plots of the initial positions of the surface-layer atoms (near the adatom clusters) and their displacements in the surface plane are shown in Figs. 7(a)–7(c). Note that the dimensions of these plots are the same and the displacements have been multiplied by a factor of 5. Also, the mean features shown in these plots are also seen in the analogous plots for Pd and Ni adatoms. Notably, the displacements are only slightly larger for Ni adatoms, in line with the similar relaxation energies for Ni and Pt clusters [Figs. 6(a) and 6(c)], and are smaller by about

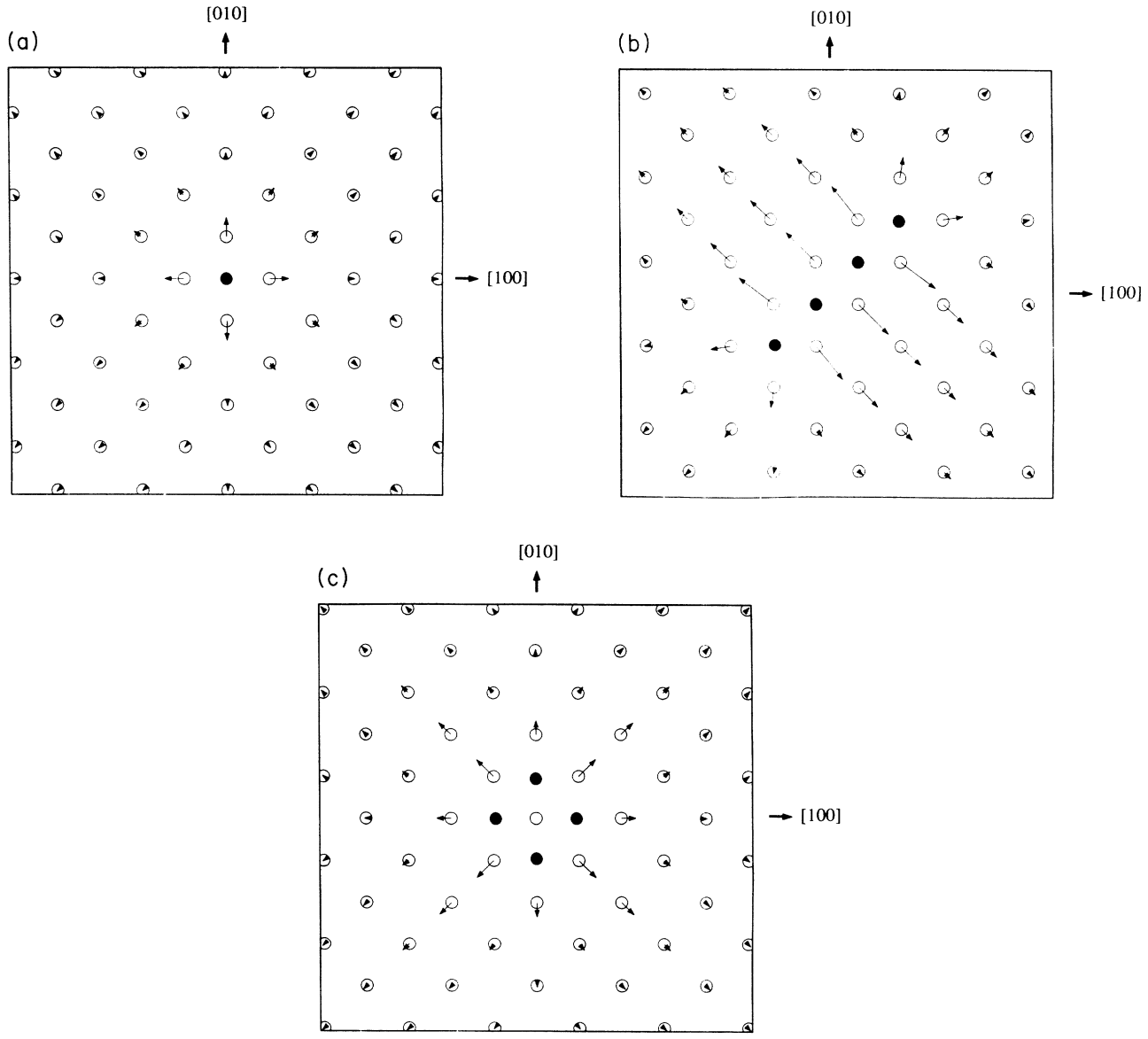

FIG. 7. Displacements of the first-layer substrate atoms, as viewed from above, near (a) a single Pt adatom, (b) a four-adatom Pt chain, and (c) a four-adatom Pt island. The open circles mark the initial positions of the substrate atoms, the arrows show their displacements multiplied by a factor of 5, and the solid circles mark the relaxed positions of the adatoms. The lengths along the edges of the plot are 20 Å.

25% for Pd adatoms, in line with the smaller relaxation energies of Pd clusters with respect to Pt clusters (Figs. 6(a) and 6(b)].

In Fig. 7(a), we see that the atoms in the surface layer relax away from a single atom. The atom nearest to the adatom is displaced by about 0.18 Å in the surface plane and by about 0.08 Å outward from the surface. In Fig. 7(b), we see even larger displacements for the surface-layer atoms near a chain of four adatoms. The atom next to the center of the chain is displaced by about 0.39 Å in the surface plane and by about 0.13 Å outward from the surface. In Fig. 7(c), we see that the surface-layer atom in the center of a square of four adatoms is unable to relax in the surface plane. Instead, it relaxes inward by about 0.21 Å. This is a common feature of the substrate relaxations from close-packed islands. The rest of the surface-layer atoms relax away from the island, however, the displacements are smaller than we saw for the four-adatom chain. The atom nearest to a side of the square is displaced by about 0.23 Å in the surface and by about 0.09 Å outward from the surface.

While we have shown only the relaxations of the surface-layer atoms, there are also relaxations in deeper layers. These are especially pronounced for chains where the second-layer atoms, located directly below the adatoms, move toward the adatoms. In fact, for the four-adatom chain, the separation between these second-layer atoms and the adatoms is only 2.80 Å, which is only slightly larger than the first near-neighbor separation in bulk Pt (2.77 Å). This suggests that these atoms have formed direct bonds with the adatoms. For the four-adatom island, in contrast, upward movement of the second-layer atoms, located directly below the adatoms, is inhibited by the presence of the central surface-layer atom.

C. Adatom interactions

As we showed earlier, the predicted stable configurations are chains for Ni, and are mostly islands for Pt and Pd. This difference naturally leads one to expect that the interactions among Ni adatoms are different than among either Pt or Pd adatoms. In fact, since the substrate relaxations are similar for Pt, Pd, and Ni clusters, we expect that the interactions among Ni adatoms on a frozen substrate should also be different than among either Pt or Pd adatoms on a frozen substrate.

With this observation, in Fig. 8 we show the important adatom interactions extracted from cluster calculations performed on a frozen substrate.[32] We note first of all that the interactions for Pt and Pd are similar. Both have a dominant first near-neighbor attractive pair interaction which leads to a rapid increase in the energy difference between chains and islands with the number of adatoms [see Figs. 5(a) and 5(b)]. This similarity is expected since the bulk lattice constants of Pt and Pd differ by less than 1%. That is, Pd first near-neighbor adatoms are nearly at their bulk separation and, as such, we expect that they will have a strong attractive interaction.

In contrast to Pd, the bulk lattice constant of Ni is about 10% smaller than that of Pt. This means that Ni

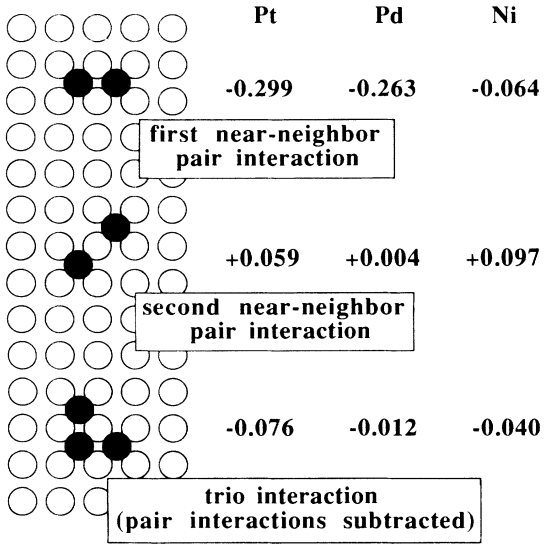

FIG. 8. The important adatom interactions, in eV, on a frozen substrate. The pair interactions are simply the pair binding energies. The triplet interaction consists of the relevant pair interactions subtracted from the triplet binding energy.

first near-neighbor adatoms are at a larger separation than in bulk Ni and, accordingly, we expect that their attractive interaction is weakened. In Fig. 8, we see that the Ni first near-neighbor pair interaction is indeed much smaller than those of Pt and Pd. Also, the Ni first near-neighbor pair interaction does not dominate the other interactions as is the case for Pt and Pd. Because of this, we do not see the rapid increase in the energy difference between chains and islands that we saw for Pt and Pd [see Fig. 5(c)]. Instead, the energies of chains and islands are similar.

As we noted in the preceding section, chains have larger relaxation energies than islands. For Ni, this feature together with the similarity of the energies of chains and islands on a frozen substrate [Fig. 5(c)] leads to chains being stabilized with respect to islands on the relaxed substrate. For Pt and Pd, the rapid increase in the energy difference between chains and islands on a frozen substrate [Figs. 5(a) and 5(b)] slightly over compensates for the larger relaxation energies of chains. This results in islands being stable with respect to chains for large clusters on a relaxed substrate.

Before concluding, we briefly report another aspect of adatom interactions which we have investigated; the long-ranged interaction of a pair of adatoms due to distortion of the substrate. This type of interaction has been treated analytically by Lau and Kohn[33] using elasticity theory. They report that the interaction energy for an identical pair of adatoms on an elastically isotropic substrate is repulsive, and that it has a C/r^3 dependence on the separation distance r of the adatoms. The interaction strength C is a function of the elastic constants of the substrate material and Lau and Kohn estimate that it is roughly 15 eV Å^3 for a metal. We peformed a series of calculations to determine the interaction energies for ada-

tom pairs given by

$$E_I=[(E_p-E_{\text{slab}})-2(E_1-E_{\text{slab}})]_{\text{relaxed slab}} -[(E_P-E_{\text{slab}})-2(E_1+E_{\text{slab}})]_{\text{frozen slab}}\ , \quad (5)$$

where E_P is the total energy of the slab with adatom pair, the first term is the pair (binding) energy on a relaxed substrate, and the second term is the pair (binding) energy on a frozen substrate. Note that the pair (binding) energies on a frozen substrate were negligible for separations greater than about 4 Å. This illustrates the short-ranged nature of adatom-adatom interactions within the EAM (as mentioned in Sec. II A).

For adatom pairs oriented along the [110] direction, for example, we found that the interaction energies have a C/r^3 dependence for r greater than about 10 Å. These interactions are repulsive and the values of C are of the same order as the estimate given by Lau and Kohn: 20 eV Å^3 for Pt adatoms, 11 eV Å^3 for Pd adatoms, and 23 eV Å^3 for Ni adatoms. In addition, we find that the interaction strength depends on the orientation of the adatom pair. The strongest interaction occurs for [110] orientation and the weakest occurs for [100] orientation. The origin of this orientation dependence is evident from the plot of the displacements of the surface-layer atoms near a single adatom [Fig. 7(a)]. The displacements are greater along the ⟨110⟩ directions than along the ⟨100⟩ directions, and accordingly, we expect that the interaction between a pair of adatoms will be stronger when they are oriented along the [110] direction.

IV. SUMMARY

In summary, we have reported on EAM calculations of the stable configurations of small Pt, Pd, and Ni adatom clusters on Pt(001). We want to point out some of the trends among the three types of adatoms. The interactions among Pt and Pd adatoms on a frozen substrate are similar in that the first near-neighbor pair interactions are attractive and dominate the other interactions. For Ni adatoms on a frozen substrate, the first near-neighbor pair interaction is also attractive, however, it is much smaller than those of Pt and Pd and has about the same magnitude as the second near-neighbor pair interaction and the triplet interaction. These interactions lead to islands being stable with respect to chains for Pt and Pd adatoms on a frozen substrate, while chains and islands have similar energies for Ni adatoms on a frozen substrate. For all three types of adatoms, relaxation energies are larger for chains than for islands by about a factor of 2. However, in this instance Pt and Ni have similar relaxation energies, while those of Pd are smaller by a factor of about 2. Nevertheless, the predicted stable configurations for Pt and Pd are similar on a relaxed substrate while those for Ni are different.

It appears that the description of adatom energetics provided by the EAM is quite good for Pt on Pt(001) as evidenced by the agreement with experimentally observed cluster configurations. The preliminary experimental results for Pd on Pt(001) indicate that the EAM may also provide a good description for this chemisorption system. On the other hand, to our knowledge there have not been any observations of Ni cluster configurations on Pt(001).

ACKNOWLEDGMENTS

The authors wish to thank Dr. S. M. Foiles of Sandia National Laboratories, Livermore, for his helpful comments at various stages of this work, and Dr. G. L. Kellogg of Sandia National Laboratories, Albuquerque, for his helpful comments and for sharing his most recent experimental results with us. This work was supported by the U.S. Department of Energy, Office of Basic Energies Sciences, Division of Materials Sciences.

[1]D. R. Tice and D. W. Basset, Thin Solid Films **20**, S37 (1974).
[2] D. W. Basset, Thin Solid Films **48**, 237 (1978).
[3]H. W. Fink and G. Ehrlich, Surf. Sci. **110**, L611 (1981).
[4]P. R. Schwoebel and G. L. Kellogg, Phys. Rev. Lett. **61**, 578 (1988).
[5]P. R. Schwoebel, S. M. Foiles, C. M. Bisson, and G. L. Kellogg, Phys. Rev. B **40**, 10 639 (1989).
[6]P. W. Anderson, Phys. Rev. **124**, 41 (1961).
[7]T. B. Grimley, Proc. Phys. Soc. London **90**, 751 (1967).
[8]T. L. Einstein and J. R. Schreiffer, Phys. Rev. B **7**, 3629 (1973).
[9]T. L. Einstein, CRC Crit. Rev. Solid State Phys. Mater. Sci. **7**, 261 (1978).
[10]R. Car and M. Parrinello, Phys. Rev. Lett. **55**, 2471 (1985); **60**, 204 (1988); M. C. Payne, J. D. Joannopoulos, D. C. Allan, M. P. Teter, and D. H. Vanderbilt, *ibid.* **56**, 2656 (1986); C. Woodward, B. I. Min, R. Benedek, and J. Garner, Phys. Rev. B **39**, 4853 (1989).
[11]P. J. Feibelman, Phys. Rev. B **35**, 2626 (1987); **33**, 719 (1986); Phys. Rev. Lett. **54**, 2627 (1985); J. Chem. Phys. **81**, 5864 (1984); A. R. Williams, P. J. Feibelman, and N. D. Lang, Phys. Rev. B **26**, 5433 (1982).
[12]M. S. Daw and M. I. Baskes, Phys. Rev. B **29**, 6443 (1984).
[13]S. M. Foiles, M. I. Baskes, and M. S. Daw, Phys. Rev. B **33**, 7983 (1986).
[14]M. S. Daw, Phys. Rev. B **39**, 7441 (1989).
[15]S. M. Foiles, Surf. Sci. **191**, L779 (1987).
[16]M. S. Daw, Surf. Sci. **166**, L161 (1986).
[17]M. S. Daw and S. M. Foiles, Phys. Rev. Lett. **59**, 2756 (1987).
[18]S. M. Foiles, Phys. Rev. B **32**, 7685 (1985).
[19]S. M. Foiles, in *Surface Segregation Phenomena,* edited by P. A. Dowben and A. Miller (CRC, Boca Raton, 1990).
[20]S. M. Foiles, Surf. Sci. **191**, 329 (1987).
[21]M. S. Daw and S. M. Foiles, in *Second International Conference on the Structure of Surfaces* (Springer-Verlag, Amsterdam, 1987).
[22]S. M. Foiles, Phys. Rev. B **32**, 3409 (1985).
[23]J. A. Moriarty, Phys. Rev. B **38**, 3199 (1988).
[24]P. Nordlander and S. Holmstrom, Surf. Sci. **149**, 443 (1985).
[25]A. G. Eguiluz, D. A. Campbell, A. A. Maradudin, and R. F. Wallis, Phys. Rev. B **30**, 5449 (1984).
[26]J. P. Muscat, Phys. Rev. B **33**, 8136 (1986).
[27]R. Fletcher and C. M. Reeves, Comput. J. **7**, 149 (1964).

[28]P. R. Norton, J. A. Davies, D. K. Creber, C. W. Sitter, and T. E. Jackson, Surf. Sci. **108**, 205 (1981).
[29]K. Heinz, E. Lang, K. Strauss, and K. Muller, Surf. Sci. **120**, L401 (1982).
[30]G. L. Kellogg (private communication).
[31]G. L. Kellogg and P. J. Feibelman, Phys. Rev. Lett. **64**, 3143 (1990).
[32]Note that the first near-neighbor pair interactions are attractive while the second near-neighbor pair interactions are repulsive. This type of behavior was discussed in Sec. II A in terms of the effective two- and three-atom interactions [Eqs. 2(a) and 2(b)].
[33]K. H. Lau and W. Kohn, Surf. Sci. **65**, 607 (1977).